



Wind Energy Resource Maps of Hawaii

Prepared for:

**Hawaii Department of Business,
Economic Development, and Tourism
Strategic Industries Division
PO Box 2359
Honolulu, Hawaii 96804**

Prepared by:

AWS Truewind, LLC
CESTM, 255 Fuller Road
Albany, New York 12203

June 30, 2004

TABLE OF CONTENTS

LIST OF TABLES.....	II
LIST OF FIGURES.....	III
EXECUTIVE SUMMARY.....	IV
1. INTRODUCTION.....	1
2. DESCRIPTION OF THE MESOMAP SYSTEM.....	1
3. IMPLEMENTATION OF MESOMAP FOR THIS PROJECT	4
4. VALIDATION	5
5. WIND MAPS	9
6. GUIDELINES FOR USE OF THE MAPS	11

LIST OF TABLES

Table 1. Range of Surface Roughness Values for Leading Land Cover Types4
Table 2. Map Validation7

LIST OF FIGURES

Figure 1. Scatter plots of predicted and measured/extrapolated mean wind speed and power in Hawaii.....8

EXECUTIVE SUMMARY

This report describes a wind-mapping project conducted by AWS Truewind for the Hawaii Department of Business, Economic Development, and Tourism (DBEDT). Using the MesoMap system, AWS Truewind has produced maps of mean wind speed in Hawaii for heights of 30, 50, 70, and 100 m above ground, as well as maps of wind power at 50 m. AWS Truewind has also produced data files of the predicted wind speed frequency distribution and speed and energy by direction. The maps and data files are provided on a WindView CD with ArcReader software, which enables users to view, print, copy, and query the maps and wind rose data.

The MesoMap system consists of an integrated set of atmospheric simulation models, databases, and computers and storage systems. At the core of MesoMap is MASS (Mesoscale Atmospheric Simulation System), a numerical weather model, which simulates the physics of the atmosphere. MASS is coupled to a simpler wind flow model, WindMap, which is used to refine the spatial resolution of MASS and account for localized effects of terrain and surface roughness. In this project, the MASS model was run on a grid spacing of 1.2 km and WindMap on a grid spacing of 200 m.

In collaboration with the National Renewable Energy Laboratory, AWS Truewind validated the wind maps using data from 99 stations located throughout the islands. The data were first extrapolated to a height of 50 m. On average, the predicted wind speeds were 0.2 m/s below the observed/extrapolated values. The root-mean-square discrepancy between the predicted and measured/extrapolated speeds was 0.9 m/s, or about 11% of the average speed for all stations. After accounting for uncertainty in the data, we estimated the map error margin to be 0.7 m/s, or 9%. This is somewhat larger than the 5-7% error typically found in MesoMap projects. The larger error margin is due in part to the wide variability of the wind resource in the islands and the importance of mesoscale circulations and topographic channeling, particularly on the island of Hawaii. In addition, the error margin may be somewhat overstated because some of the data may not be reliable.

After discussions with NREL, the maps were adjusted in several areas to reduce the errors. The main adjustments were along the south coast of Oahu, the northern and southern coasts of Kauai, the northern coast of Molokai, and the northwestern and southeastern coasts of Hawaii.

The maps indicate that Hawaii has a very complex wind resource. The islands are immersed in the northeasterly trade winds. Since the trade winds are relatively shallow and capped by a temperature inversion, they are easily blocked and channeled by the mountains of the major islands. Such channeling results in excellent winds between the islands, such as between Molokai and Maui, with mean speeds ranging from 8 to 12 m/s at 50 m. Coastal points that are exposed to the channeled winds (such as Koko Head on Oahu) are consequently very windy. Channeling between and around mountains on the same island also occurs; examples include high winds around Maalaea Bay, Maui, and Kahua Ranch, Hawaii. Conversely, mountain blocking is predicted to result in a relatively modest wind resource to the northeast and southwest coasts of the major islands, and on the highest mountaintops.

1. INTRODUCTION

The Hawaii Department of Business, Economic Development, and Tourism (DBEDT) is interested in assessing the wind resource of Hawaii and finding suitable sites for wind energy projects. Conventional field techniques of wind resource assessment can be time consuming, and often depend heavily on local meteorological expertise as well as the availability of reliable and representative wind measurements. Conventional wind flow models, on the other hand, have often proven inaccurate in complex wind regimes, and even in moderate terrain their accuracy can decline substantially with distance from the nearest available reference mast.

Mesoscale-microscale modeling techniques offer a solution to these challenges. By combining a sophisticated numerical weather model capable of simulating the general wind patterns with a microscale wind flow model responsive to local terrain and surface conditions, they enable the mapping of wind resources over large regions with much greater accuracy than has been possible in the past. In addition, they do not require surface wind data to make reasonably accurate predictions. While on-site measurements are still required to confirm the predicted wind resource at any particular location, mesoscale-microscale modeling can greatly reduce the time and cost to identify and evaluate potential wind project sites.

Having introduced the MesoMap system in the late 1990s, AWS Truewind (formerly Truewind Solutions) has become the world leader in the development of mesoscale-microscale mapping techniques. In the past five years, MesoMap has been applied in nearly 30 countries on four continents. In North America alone, MesoMap has been used to map over 30 US states and several provinces of Canada and states of Mexico.

The objective of the current project was to use MesoMap to create high-resolution wind resource maps of Hawaii and to provide wind resource data in a format enabling the DBEDT to assess potential sites in a GIS. These objectives have been met. In the following sections, we describe the MesoMap system and mapping process in detail; how MesoMap was applied in this project; the validation process and results; the final wind maps and data files; and guidelines for the use of the maps.

2. DESCRIPTION OF THE MESOMAP SYSTEM

The MesoMap system has three main components: models, databases, and computer systems. These components are described below.

2.1. Models

At the core of the MesoMap system is MASS (Mesoscale Atmospheric Simulation System), a numerical weather model that has been developed over the past 20 years by AWS Truewind partner MESO, Inc., both as a research tool and to provide commercial weather forecasting services. MASS simulates the fundamental physics of the atmosphere including conservation of mass, momentum, and energy, as well as the moisture phases, and it contains a turbulent kinetic energy module that accounts for the effects of viscosity and thermal stability on wind shear. As a dynamical model, MASS simulates the evolution of atmospheric conditions in time steps as short as a few seconds. This creates

great computational demands, especially when running at high resolution. Hence MASS is usually coupled to a simpler but much faster program, WindMap, a mass-conserving wind flow model. Depending on the size and complexity of the region and requirements of the client, WindMap is used to improve the spatial resolution of the MASS simulations to account for the local effects of terrain and surface roughness variations.

2.2. Data Sources

The MASS model uses a variety of online, global, geophysical and meteorological databases. The main meteorological inputs are reanalysis data, rawinsonde data, and land surface measurements. The reanalysis database – the most important – is a gridded historical weather data set produced by the US National Centers for Environmental Prediction (NCEP) and National Center for Atmospheric Research (NCAR). The data provide a snapshot of atmospheric conditions around the world at all levels of the atmosphere in intervals of six hours. Along with the rawinsonde and surface data, the reanalysis data establish the initial conditions as well as updated lateral boundary conditions for the MASS runs. The MASS model itself determines the evolution of atmospheric conditions within the region based on the interactions among different elements in the atmosphere and between the atmosphere and the surface. Because the reanalysis data are on a relatively coarse, 200 km grid, MASS is run in several nested grids of successively finer mesh size, each taking as input the output of the previous nest, until the desired grid scale is reached. This is to avoid generating noise at the boundaries that can result from large jumps in grid cell size. The outermost grid typically extends several thousand kilometers.

The main geophysical inputs are elevation, land cover, vegetation greenness (normalized differential vegetation index, or NDVI), soil moisture, and sea-surface temperatures. The global elevation data normally used by MesoMap were produced by the US Geological Survey in a gridded digital elevation model, or DEM, format from a variety of data sources.¹ The US Geological Survey, the University of Nebraska, and the European Commission's Joint Research Centre (JRC) produced the global land cover data in a cooperative project. The land cover classifications are derived from the interpretation of Advanced Very High Resolution Radiometer (AVHRR) data – the same data used to calculate the NDVI. The model translates both land cover and NDVI data into physical parameters such as surface roughness, albedo, and emissivity. The nominal spatial resolution of all of these data sets is 1 km. Thus, the standard output of the MesoMap system is a 1 km gridded wind map. However, much higher resolution maps can be produced where the necessary topographical and land cover data are available. In the United States, the resolution is typically 100 to 400 m.

2.3. Computer and Storage Systems

The MesoMap system requires a very powerful set of computers and storage systems to produce wind resource maps at a sufficiently high spatial resolution in a reasonable amount of time. To meet this need AWS Truewind has created a distributed processing

¹The Shuttle Radar Topographic Mission (SRTM) 30 arc-second data base the principal source for the global 1 km elevation data.

network consisting of 94 Pentium II processors and 3 terabytes of hard disk storage. Since each day simulated by a processor is entirely independent of other days, a project can be run on this system up to 94 times faster than would be possible with any single processor. To put it another way, a typical MesoMap project that would take two years to run on a single processor can be completed in just one week.

2.4. The Mapping Process

The MesoMap system creates a wind resource map in several steps. First, the MASS model simulates weather conditions over 366 days selected from a 15-year period. The days are chosen through a stratified random sampling scheme so that each month and season is represented equally in the sample; only the year is randomized. Each simulation generates wind and other weather variables (including temperature, pressure, moisture, turbulent kinetic energy, and heat flux) in three dimensions throughout the model domain, and the information is stored at hourly intervals. When the runs are finished, the results are compiled into summary data files, which are then input into the WindMap program for the final mapping stage. The two main products are usually (1) color-coded maps of mean wind speed and power density at various heights above ground and (2) data files containing wind speed and direction frequency distribution parameters. The maps and data can then be compared with land and ocean surface wind measurements, and if significant discrepancies are observed, adjustments to the wind maps can be made.

2.5. Factors Affecting Accuracy

In our experience, the most important sources of error in the wind resource estimates produced by MesoMap are the following:

- Finite grid scale of the simulations
- Errors in assumed surface properties such as roughness
- Errors in the topographical and land cover data bases

The finite grid scale of the simulations results in a smoothing of terrain features such as mountains and valleys. For example, a mountain ridge that is 2000 m above sea level may appear to the model to be only 1600 m high. Where the flow is forced over the terrain, this smoothing can result in an underestimation of the mean wind speed or power at the ridge top. Where the mountains block the flow, on the other hand, the smoothing can result in an overestimation of the resource as the model understates the blocking effect. The problem of finite grid scale can be solved by increasing the spatial resolution of the simulations, but at a cost in computer processing and storage.

Errors in the topographical and land cover data can obviously affect wind resource estimates. While elevation data are usually reliable, errors in the size and location of terrain features nonetheless occur from time to time. Errors in the land cover data are more common, usually as a result of the misclassification of aerial or satellite imagery. It has been estimated that the global 1 km land cover database used in the MASS simulations is about 70% accurate. Where possible, more accurate and higher resolution land cover databases should be used in the WindMap stage of the mapping process to correct errors introduced in the MASS simulations. In the United States, we use a 30 m

gridded Landsat-derived land cover database for this purpose; a similar 250 m database, called Corine, is available for most of Western Europe.

Even if the land cover types are correctly identified, there is uncertainty in the surface properties that should be assigned to each type, and especially the vegetation height and roughness. The forest category, for example, may include many different varieties of trees with varying heights and density, leaf characteristics, and other features that affect surface roughness. Cropland may be virtually devoid of trees and buildings, or it may have many windbreaks. Uncertainties like these can be resolved only by acquiring more information about the area through aerial photography or field observation. However this is not practical when (as in this project) the area being mapped is very large.

3. IMPLEMENTATION OF MESOMAP FOR THIS PROJECT

The standard MesoMap configuration was used in this project. MASS was run on the following nested grids:

- First (outer) grid level: 30 km
- Second (intermediate) grid level: 12 km
- Third (intermediate) grid level: 4.8 km
- Fourth (inner) grid level: 1.2 km (1.4 km over Hawaii)

The usual geophysical and meteorological inputs were used. The WindMap program adjusted the wind resource estimates to reflect local topography and surface roughness changes on a grid spacing of 200 m. For the topographical data, we used the National Elevation Dataset, a digital terrain model produced on a 30 m grid by the US Geological Survey (USGS). For the land cover, we used the USGS Land Use Land Cover (LULC) data, which are based on the manual interpretation of aerial photography. It was produced by the USGS at 1:250,000 scale.² Both data sets are judged to be of high quality.

In converting from land cover to surface roughness, the roughness length values shown in Table 1 were assumed. We believe these values to be typical of conditions in Hawaii. However the actual roughness could vary a good deal within each class, and is a source of substantial uncertainty in the wind mapping results.

Table 1. Range of Surface Roughness Values for Leading Land Cover Types

Description	Roughness (m)
Rangeland	0.03
Cropland/Shrubland	0.05
Urban or Built-Up	0.3
Forest	0.9

² Information on the Land Use Land Cover data set can be found at the following web address: <http://edcwww.cr.usgs.gov/products/landcover/lulc.html>. Information on the National Elevation Dataset (NED) can be found at <http://edcwww.cr.usgs.gov/products/elevation/ned.html>.

The roughness is not the only surface property with a direct effect on near-surface wind speeds. Where there is dense vegetation the wind can skim along the vegetation canopy, thereby displacing the flow above the ground and reducing the speed observed at a fixed height above ground. The displacement height is defined as the height at which the wind speed becomes zero in the logarithmic shear formula. The shear formula is as follows:

$$\frac{v_2}{v_1} = \frac{\ln\left(\frac{z_2 - d}{z_0}\right)}{\ln\left(\frac{z_1 - d}{z_0}\right)}$$

Here, d is the displacement height, z_1 and z_2 are two different heights at which the speed v is measured, and z_0 is the surface roughness (generally much less than z_2 and z_1). Note that according to this formula, when $z_2 = d + z_0$, $v_2 = 0$.

The displacement height is usually estimated to be about two-thirds to three-fourths the maximum vegetation height. For this project, we assumed that the displacement height was 10 times the surface roughness length, which was in turn defined to be approximately 7.5% of the vegetation height. For deciduous forests with a roughness length of 0.9 m, this resulted in a displacement height of 9 m.

The effect of displacement height is to reduce the wind speed observed near the ground and to increase the apparent wind shear measured with respect to ground level. It can also reduce the wind speed measured in small clearings, since the ground appears to be in a “hole” at a depth d below the vegetation canopy. The impact of this hole on wind speed diminishes as the clearing becomes large enough for the flow to reach equilibrium with the new effective ground height. As a rule of thumb, the clearing width should be at least 20 times the displacement height for the effect to be negligible at the center of the clearing, but under some conditions the minimum width should be even larger.

4. VALIDATION

The wind resource maps were initially produced without reference to surface wind measurements. AWS Truewind and NREL then validated the wind maps by comparing the predicted speed against data from 99 stations. Consulting meteorologists Richard L. Simon and Lucille Olszewski contributed data and insights to the analysis. Thirteen stations were at airports. There was also a number of automated weather stations (such as RAWS and Coast Guard), as well as over 50 tall towers (towers over 20 m in height), many of which were instrumented specifically for wind resource assessment. Many of the stations, particularly the tall towers, were clustered in areas that have been the subject of extensive wind resource assessment in the past. The data in those cases were aggregated to avoid biasing the error statistics.

The validation was carried out in the following steps:

1. Station locations were verified and adjusted, if necessary, by comparing the quoted elevations and station descriptions against the elevation and land cover

maps. Where there was an obvious error in position, the station was moved to the nearest point with the correct elevation and surface characteristics.

2. The observed mean speed and wind power density were extrapolated to a common reference height of 50 m using the power law. In most cases, the shear exponent had to be estimated, since multi-level shear data were not available. The assumed shear values ranged from 0.10 to 0.17, with the lower values generally applied along coasts and on mountaintops. The power shear exponent was assumed to be $3(\alpha-0.02)$, where α was the speed shear exponent. This relationship assumes that the speed frequency distribution becomes narrower with increasing height above ground.
3. The error margin for each data point was then estimated as a function of two factors: the tower height and the number of years of measurement. The tower height enters the equation because of uncertainty in the wind shear. We assumed an error margin in the shear exponent of 0.03. The number of years of data affects the uncertainty because winds recorded over a short period may not be representative of long-term conditions. A rule of thumb is that a mean speed based on one year of data will be within 10% of the true long-term mean with 90% confidence. This translates into a standard error of 6% for one year of data. We assumed that the annual mean varies randomly according to a normal distribution, and thus the error margin varies inversely with the square root of the number of years. An additional uncertainty of 3% was added to account for possible variations in the characteristics of anemometers and data loggers. These uncertainties do not account for possible errors caused by bad data, site obstructions, and other factors.
4. The various uncertainties were then combined in a least-squares sum as follows:

$$(1) e = \sqrt{0.03^2 + \left(\left(\frac{50}{H} \right)^{0.03} - 1 \right)^2 + \left(\frac{0.06}{\sqrt{N}} \right)^2}$$

where H is the height of the anemometer, and N the number of years of measurement. The uncertainty in power (in percentage terms) is assumed to be three times the uncertainty in speed, since the power varies as the cube of the speed.

5. Next, the predicted and measured/extrapolated speed and power were compared, and the map bias (map speed or power minus measured/extrapolated speed or power) was calculated for each point.

Table 2 summarizes the results. The key finding is that the root-mean-square (RMS) discrepancy in speed and power were 0.9 m/s (11% of the average observed speed) and 120 W/m² (27% of the average observed power), respectively. The wind power RMS discrepancy is larger than the wind speed discrepancy in percentage terms because the power varies as the cube of the speed.

Table 2. Preliminary Validation

	Number of Stations	Mean Bias	RMS Discrepancy	Model Error
Speed	99	-0.2 m/s (-2%)	0.9 m/s (11%)	0.7 m/s (9%)
Power	54	9 W/m ² (2%)	120 W/m ² (27%)	75 W/m ² (17%)

The RMS discrepancy reflects errors both in the model and the data, and thus tends to overstate the error of the maps alone. The model error is estimated by subtracting (in a least-squares sense) the standard error of the data (e_{DATA}) from the total RMS discrepancy (e_{TOTAL}):

$$(2) e_{MODEL} \approx \sqrt{e_{TOTAL}^2 - e_{DATA}^2}$$

This equation assumes that the errors in the model and data are random, normally distributed, and independent of one another. Using this equation, the speed error for the model alone is found to be 0.7 m/s, or 9%. The power error is 75 W/m², or 17%.

The scatter plots in Figure 1 compare the predicted and measured-extrapolated wind speed and power at 50 m height. The linear trend lines, which are forced through the origin, confirm that the map speeds are slightly higher than the observed/extrapolated speeds on average, while the map power shows less bias and a higher r^2 .

Although the agreement between model and data is not bad overall, the errors shown in Table 1 are somewhat larger than usual for MesoMap projects. (The typical model error is 5-7%.) The scatter plots suggest that the results may be affected by a few outlying data points where the model and data disagree to a much larger extent than the data error margin should allow.

Two main factors may be responsible for the higher-than-normal errors. First, the wind resource in Hawaii is exceptionally variable, with temperature-driven circulations as well as topographic channeling and blocking playing an unusually important role. Such circulations and topographic effects are difficult to simulate accurately, particularly in Hawaii, where the height of the marine inversion is a critical parameter. If the marine layer is too deep in the simulations, there is less blocking and channeling by the mountains; conversely, a too-shallow layer will result in an overestimation of these effects. Local circulations – such as downslope katabatic winds – are very sensitive to the daily temperature cycle, which is in turn sensitive to soil moisture, cloud cover, vegetation cover, and other model parameters.

Second, some of the data used in the validation may not be entirely reliable. The most curious case in the validation sample is Moomomi, on northern Molokai island, where the observed speed was nearly 12 m/s, while the map speed was only 7.7 m/s. We are skeptical of this data point, since records show that a small wind project in the Moomomi area, consisting of three Vestas wind turbines, produced a net capacity factor of only 29% with 96% availability over a two-year period. The Moomomi data, if correct, may be unrepresentative of the area. Removing this station from the validation sample reduces

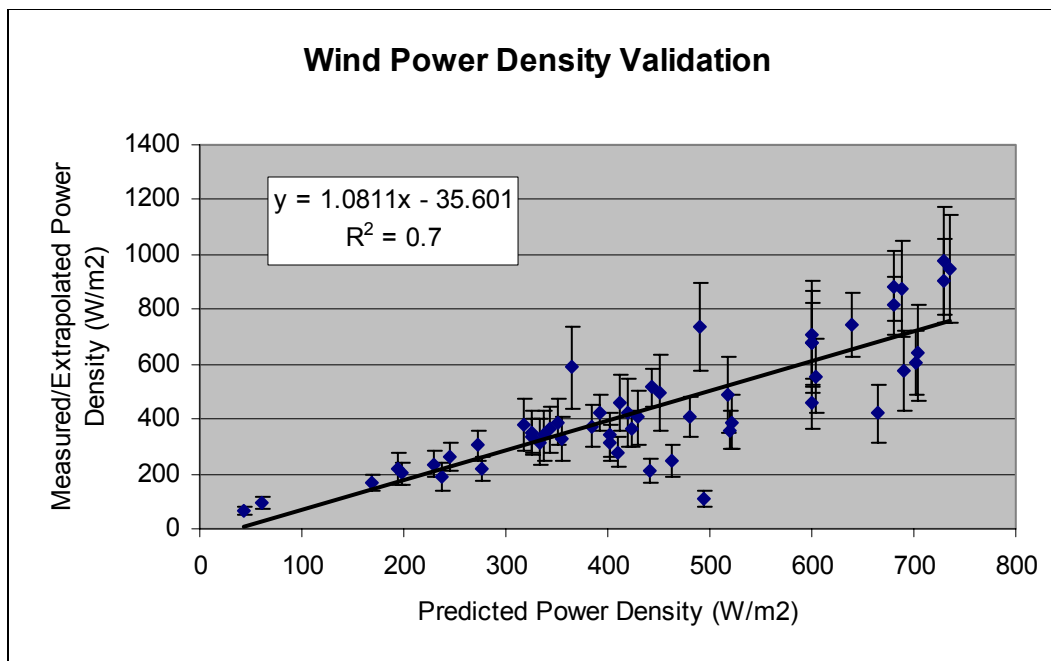
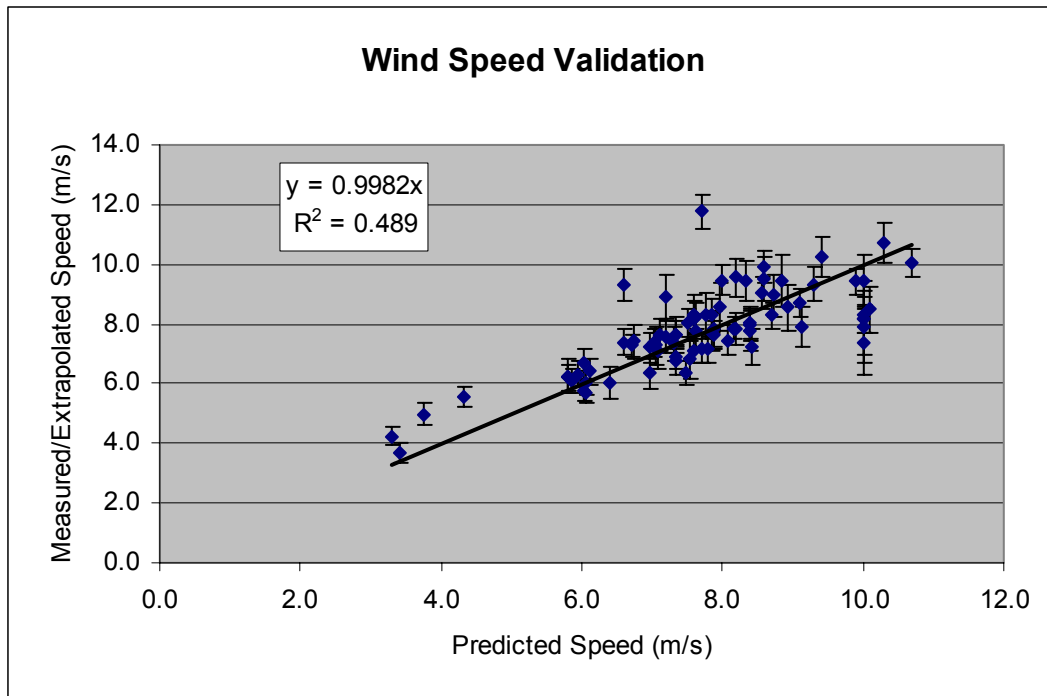


Figure 1. Scatter plots of predicted and measured wind speeds in Hawaii at 50 m (top), and the same for wind power density (bottom). The error bars reflect period of record, tower height, and anemometer sensitivity, as described in the text. The trend lines are forced through the origin.

the apparent model speed error from 9% to 7%, which is now within the normal MesoMap range.

Other outlying data points, on the other hand, probably represent real model errors. An example is Upolu Point, on the northwestern coast of Hawaii, where the model predicted

the (rather low) wind speed fairly accurately, but greatly overestimated the wind power density. This indicates that there were a few occasions in the simulations when the model created a very strong wind off the ridge to the northeast which did not in fact occur. This could reflect errors in the temperature gradient or the height of the marine inversion.

After reviewing and discussing the validation results, NREL and AWS Truewind agreed on adjustments in several areas. The wind speed and power were increased along the northern coast of Kauai but decreased along the southern coast. The speed and power were increased along the southern coast of Oahu, and likewise around Kahului, on Maui; around Moomomi and the Kalaupapa Peninsula, on Molokai; and around Lalamilo Wells, on Hawaii. The wind power was reduced along the southwestern coast of Maui, as well as the northwestern coast of Hawaii. Finally, reductions were applied at South Point, on Hawaii, and along part of the southeastern Hawaii coast.

5. WIND MAPS

The accompanying maps, which incorporate the adjustments described in the previous section, show the predicted mean annual wind speed in Hawaii at heights of 30, 50, 70, and 100 m. A map of mean annual wind power density at 50 m is also provided; this can be compared directly with the previous wind resource map of the state from the national wind resource atlas.³

The mean speed and power describe different aspects of the wind resource, and both can be useful in different ways. The mean speed is the easiest for most people to relate to and is consequently the most widely used. However, it does not directly measure the power-generation potential in the wind. Some experts regard the mean wind power, which depends on the air density and the cube of the wind speed, as a more accurate indicator of the wind resource when assessing wind project sites. Generally speaking, commercial wind power projects using large turbines require a mean speed of at least 7 m/s or mean power of at least 400 W/m² (NREL class 4). Some small turbines are designed to operate at lower wind speeds, and may be useful at mean speeds (at 30 m height) as low as 5-6 m/s (NREL class 2 to 3).

The most obvious feature of the maps is the remarkable concentration of the wind resource in the channels between the major islands, including Pailolo Channel between Molokai, Lanai, and Maui, Alenuihaha Channel between Maui and the Big Island of Hawaii, and Kaiwi Channel between Oahu and Molokai. The underlying mechanism is the effect of the high mountain ranges of the islands on the prevailing northeasterly trade winds. A characteristic feature of trade winds is that they are relatively shallow, extending perhaps 1000-2000 m above the ocean surface, and are capped by a temperature inversion that prevents the flow from rising very high over obstacles. Finding itself blocked by high mountains, the air mass seeks alternative paths, resulting in a concentration of the flow through channels. The intensity of the wind is a function of the width of the channel and the degree of blocking. The tallest mountains are found on Molokai, Maui, and the Big Island, and thus the strongest winds are found in the channels between and around these islands.

³ *Wind Energy Resource Atlas of the United States* (Department of Energy, 1986).

The mountain blocking and channeling create more subtle features of the wind resource as well. Consider the pattern of winds through the center of Maui from the town of Pauwela on the north coast to Maalaea on the south coast. This area lies in a gap between Puu Ula Ula (Haleakala Peak) on the east side of the island and Puu Kukui (West Maui Mountains) on the west. The northeasterly wind is initially forced to come around the north slopes of Haupakea, resulting in a concentration of the resource around Pauwela. As it crosses to the southern side of the island, the wind is once again forced around the southern slopes of Puu Kukui. Like a slingshot, the flow accelerates towards a zone of low pressure created behind Puu Kukui, resulting in a predicted mean wind speed of around 10 m/s within and to the south of Maalaea Bay. Similar, though less intense, features are visible along the northern coast of Molokai, near Makakilo City on Oahu, and between Mauna Loa and Mauna Kea on Hawaii.

On the island of Lanai, the maps show an area of good wind resource in what seems a surprising location: the western end of the island, on the southwestern slope of Kanepuu leading down to the shore. Why here, and not the much higher terrain at the eastern end of the island? Whereas the eastern end of the island is in the shadow of Puu Kukui on Maui, the resource at the western end is effectively within the influence of Pailolo Channel. Although the surface wind speed is diminished as the flow comes over the hills at the western end of the island, it picks up again as the air mass “feels” the low pressure created behind the hills and rushes back down to the sea.

Other areas benefiting from the Pailolo Channel flow include the finger ridges stretching northward from Puu Kukui to the western tip of Maui, and similar ridges extending from Keanakoholua Ridge down to the southeastern shore of Molokai. Similar features exist on Oahu, including Kahuku Point and Kaena Point on the western end of the island, and the ridges extending down to Koko Head and Diamond Head on the eastern end; and on Hawaii, at Upolu Point and South Point. On Hawaii, channeling through a gap in the mountains creates a very good wind resource near Lalamilo Wells.

The concentration of the resource in these channels leaves deficits elsewhere. The deficit is most apparent on the upwind (ENE) and downwind (WSW) sides of the major islands. These areas offer fewer prospects for wind energy than elsewhere. In addition, most ridges of 1500 m and higher elevation have a moderate wind resource (7-8 m/s) compared to ridges of lower elevation. The reason is that they reach too high into the atmosphere to benefit greatly from the shallow trade winds. This applies especially to the mountains of Maui and the Big Island of Hawaii.

On Oahu, on the other hand, the main ridges have peak elevations of only about 800 m. This is not too high to block the energetic trade winds, and thus the ridges, which are oriented perpendicular to the prevailing flow, are able to compress and accentuate the winds aloft to a considerable degree. The main ridgelines along Oahu are predicted to have a very good resource ranging up to around 10 m/s. Still, the highest points along these ridges are not generally the most favored; lower elevations and especially passes, such as Kolekole Pass, are expected to be somewhat windier, or at least no less windy, than the peaks.

6. GUIDELINES FOR USE OF THE MAPS

The following are guidelines for interpreting and adjusting the wind speed estimates in the maps, to be used in conjunction with the accompanying ArcReader CD. The ArcReader CD allows users to obtain the “exact” wind speed value at any point, and it provides the elevation and surface roughness data used by the model, which are needed to apply the adjustment formulas given below.

1. The maps assume that all locations are free of obstacles that could disrupt or impede the wind flow. “Obstacle” does not apply to trees if they are common to the landscape, since their effects are already accounted for in the predicted speed. However, a large outcropping of rock or a house would pose an obstacle, as would a nearby shelterbelt of trees or a building in an otherwise open landscape. As a rule of thumb, the effect of such obstacles extends to a height of about twice the obstacle height and to a distance downwind of 10-20 times the obstacle height.
2. Generally speaking, points that lie above the average elevation within a 400×400 m grid cell will be somewhat windier than points that lie below it. A rule of thumb is that every 100 m increase in elevation will raise the mean speed by about 0.5 m/s. This formula is most applicable to small, isolated hills or ridges in flat terrain.
3. The mean wind speed at a location could be affected by the roughness of the land surface – determined mainly by vegetation cover and buildings – up to several kilometers away. If the roughness is much lower than that assumed by the model, the mean wind speed could be higher. Typical values of roughness range from 0.01 m in open, flat ground without significant trees or shrubs, to 0.1 m in land with few trees but some smaller shrubs, to 1 m or more for areas with many trees. These values are only indirectly related to the size of the vegetation.

The following equation provides an approximate speed adjustment for differences in surface roughness in the direction of the wind:

$$\frac{v_2}{v_1} \approx \frac{\log\left(\frac{300-d}{z_{01}}\right)}{\log\left(\frac{h-d}{z_{01}}\right)} \times \frac{\log\left(\frac{h-d}{z_{02}}\right)}{\log\left(\frac{300-d}{z_{02}}\right)}$$

v_1 and v_2 are the original and adjusted wind speeds at height h (in meters above ground level); z_{01} and z_{02} are the model and actual surface roughness values (in meters); and d_1 and d_2 are the corresponding displacement heights. (This equation assumes the wind is unaffected by localized roughness changes above a height of 300 m.)

As an example, suppose the surface roughness assumed by the model was 0.2 m, and the displacement 2 m, whereas the true roughness is 0.75 m and displacement 7.5 m. For $h = 50$ m, the above formula gives

$$\frac{v_2}{v_1} \approx \frac{\log\left(\frac{300 - 2}{0.2}\right)}{\log\left(\frac{50 - 2}{0.2}\right)} \times \frac{\log\left(\frac{50 - 7.5}{0.75}\right)}{\log\left(\frac{300 - 7.5}{0.75}\right)} = 0.90$$

This shows that the predicted wind speed should be reduced by about 10%.

This formula assumes that the wind is in equilibrium with the new surface roughness above the height of interest (in this case 50 m). When going from high roughness to low roughness (such as from forested to open land), the clearing should be at least 1000 m wide for the benefit of the lower roughness to be fully realized. However, when going from low to high roughness, the reduction in wind speed may be felt over a much shorter distance. For this and other reasons, the formula should be applied with care.